Journal of Power Sources 196 (2011) 6554–6558

Contents lists available at ScienceDirect

Journal of Power Sources

journal homepage: www.elsevier.com/locate/jpowsour

Short communication

Experimental triggers for internal short circuits in lithium-ion cells

Christopher J. Orendorff*, E. Peter Roth, Ganesan Nagasubramanian

Sandia National Laboratories, PO Box 5800, Albuquerque, NM 87185, United States

ARTICLE INFO

Article history:
Received 29 January 2011
Received in revised form 14 March 2011
Accepted 15 March 2011
Available online 23 March 2011

Keywords:
Lithiuim-ion cell
Battery safety
Internal short circuit

ABSTRACT

Lithium-ion cell field failures due to internal short circuits are a significant concern to the entire lithium-ion cell market from consumer electronics to electric vehicles. While the probability of these failure events occurring is estimated to be very low (1 in 5–10 million), the consequences of a cell failure due to an internal short in a high energy battery system have the potential to be catastrophic. The statistical probability of one of these events is very low and they are difficult to predict and simulate in a laboratory using some external test; which makes cell failure due to an internal short circuit a unique challenge to overcome. Several of the experiments designed to simulate internal shorts have been adopted as testing protocols across the industry; in general, they do not accurately simulate an internal short. This work highlights our efforts to experimentally trigger an internal short circuit in a lithium-ion cell.

1. Introduction

As the use of lithium-ion batteries extends from consumer electronics to higher power and higher energy vehicle and stationary utility storage applications, safety issues with these systems will become of increasing concern. Specifically, field failures due to cell internal short circuits are of a particular concern to the industry because they are difficult to detect and predict and can lead to catastrophic, spectacular cell failure [1–3]. While they can vary in nature, internal shorts can develop from a variety of sources which may include manufacturing defects (separator damage, contamination particles introduces during cell building, or weld or solder splatter at the tab/electrode connection), dissolution/deposition of electrode materials, lithium plating and dendrite formation. It is important to note that all of these can develop over time under normal use or abuse conditions.

There are numerous types of internal shorts that can occur in a cell, all of which have different consequences in terms of cell failure. There are several variables that can affect cell response to an internal short including the surface area, resistance, location within a cell, cell state-of-charge (SOC) and cell nominal capacity. Moreover, shorts can occur between the anode and cathode active materials (anode–cathode), aluminum or copper current collectors and active materials (Al-anode, Cu-cathode) or between the current collectors (Al–Cu). This matrix of possibilities has a significant impact on cell heating (localized vs. homogeneous) [4]. the amount of current passed through the short, and the severity of the subsequent cell failure. In general, Cu-cathode and anode-cathode short circuits have the highest contact resistance (»100 mΩ); which limits the current flow through the short, localized heating and the overall severity. Al–Cu shorts have very little contact resistance (<10 mΩ), but in this case the heat from the short current is readily dissipated through the cell given the high thermal conductivity of the copper current collector. The result is typically homogeneous heating throughout the cell and generally no catastrophic failure. Al-anode shorts are generally the most severe because the contact resistance is relatively low (~100 mΩ), the thermal conductivity of the aluminum current collector is not as high as copper, and the short current leads to localized heating at the short. Moreover, degradation reactions of the anode SEI occur at relatively low temperatures (80–100 °C) compared to cathode decomposition (>180 °C), leading to more heat generation and potential catastrophic failure of the cell [5]. Santhanagopalan et al. have recently reported the severity of ISCs under various conditions using a lumped electrochemical thermal numerical model and found that the most severe and potentially damaging ISCs are relatively small area (1 mm^2), have an impedance of 100 mΩ, and occur between the aluminum current collector and the lithiated graphite anode (100% SOC) [5].

Most of the internal short circuit testing developed to date involves some form of mechanical deformation of the cell to the point where a physical internal short develops. This has been demonstrated using a blunt rod to indent a cell (but stopping before it actually ruptures the cell packaging); variations of which have been developed at Underwriters Laboratory (UL) and NASA [6–8], small nail penetration [9], surface indentation or pinch test developed at Motorola [9], or the forced-internal short circuit (FISC) approach developed by the Battery Association of Japan. While these tests can be performed on production line cells in a manufacturing setting, there are some notable shortcomings including

* Corresponding author. Tel.: +1 505 844 5879; fax: +1 505 844 6972.
E-mail address: corendo@sandia.gov (C.J. Orendorff).

0378-7753/$ – see front matter © 2011 Elsevier B.V. All rights reserved.
doi:10.1016/j.jpowsour.2011.03.035

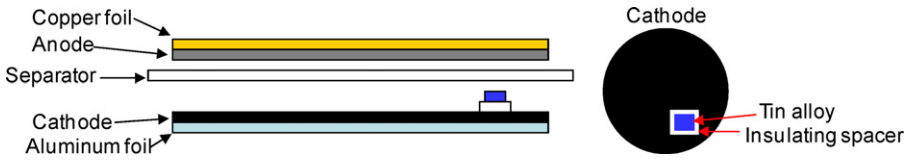

Fig. 1. Schematic of method for introducing Sn/Bi/In alloy defect structures into lithium-ion cells.

reproducibility, the inability to control the type of internal short (Al–Cu, Cathode-Cu, Anode-Cathode, etc.), restrictions on their utility based on cell configuration (wound or prismatic) and packaging (steel can or polymer pouch). One non-mechanical approach to initiate an internal short has been reported by TIAX, which relies on the dissolution and deposition of metal defect particles at the electrode surfaces with cell cycling [10]. This cycling causes dendritic metal growth at the anode electrode and an eventual internal short. Results using this approach are quite promising at emulating a true field failure and eliminating some of the shortcomings of mechanical testing. However, there remain challenges with the reproducibility of this approach and controlling the state-of-charge (SOC) of the cell at the time when the short occurs.

The object of this work is to develop an experimental approach to trigger an internal short circuit in lithium-ion cells to determine their thermal response. We are interested in triggering an internal short circuit under conditions that closely mimic field failure scenarios (ambient temperature, pressure, "normal use" conditions) and to control the type of internal short in the cell (Al–Cu, Anode-Al, Cathode–Anode, Cathode-Cu) as well as location, impedance, current path, surface area and cell SOC. This report describes the use of low-melting point metals or alloys to generate a controlled internal short. The alloy is inserted into the cell during cell building and is initially electrically insulated from the electrodes. Upon heating above the melting temperature, the liquid metal breaches the separator insulation, makes electrical contact with both electrodes and short circuits the cell internally. Choice of metal and experimental geometry are critical for implementation of this technique as the defect site must be stable in a lithium-ion electrochemical cell, not interfere with the electrochemical performance of the system, and should be applicable to any cell format (spiral wound, flat/prismatic, etc.). Our objective is to deploy this technique in 18,650 or wound prismatic cells, however, much of the initial development work is performed using 2032 coin cells.

2. Experimental

2.1. Materials

Cell electrode materials consisted either of coated electrodes provided by MSA (Mine Safety Appliances) using $LiCoO_2$ cathodes\MCMB carbon anodes or in-house coated electrodes using nickel manganese cobalt oxide ($Li(Ni_{1/3}Mn_{1/3}Co_{1/3})O_2$, NMC), cathodes provided by 3 M Corporation, and graphite carbon (G8) anode active material provided by Conoco Phillips. The electrolyte used in all of the cells was EC:EMC (3:7)\1.2 M $LiPF_6$. The lithium hexafluorophosphate ($LiPF_6$) was purchased from Hoshimoto Chemical (Japan) and the ethylene carbonate (EC)\ethylmethyl carbonate (EMC) were purchased from Kishida Chemical (Japan). N-methylpyrolidone (NMP) was used to dissolve the active material\binder mix and was purchased from Aldrich. Bismuth/tin/indium (Bi/Sn/In) low-melt temperature alloys and gallium metal samples were purchased from Atlantic Metals. Cathode and anode powders and electrodes were dried in a vacuum oven prior to use. All cell building was peformed in either inert (Ar) atmosphere on in a dry room with a dew point <−40 °C.

2.2. Methods

Cathode electrodes were prepared by mixing NMC, SAB carbon (conductive additive) and poly(vinylidene fluoride) (PVDF) binder (90:5:5 wt.%) in NMP. Blade casting of the slurry onto a carbon-coated aluminum foil current collector was used for the coin cells. A Hosen coater was used to prepare longer length electrodes for the 18,650 cells. Anode electrodes were prepared in a similar manner by mixing graphite carbon, SAB carbon, and PVDF (92:2:6 wt.%) in NMP with a copper foil current collector. Anode and cathode electrodes were vacuum dried prior to use. The 2032 coin cells were built using either (1) MSA $LiCoO_2$ and graphite or (2) 3 M NMC and Conoco Phillips graphite electrodes with Tonen V25EKD (25 μm) separator. Coating thicknesses ranged from 60 to 80 μm. All cells were flooded with 1.2 M $LiPF_6$ in EC:EMC (3:7) [wt. ratio] electrolyte. 18,650 cells (nominally 1000 mAh) were rolled using either a MicroTech or a Hosen prototype winder at the Sandia National Laboratories lithium-ion cell fabrication facility [11]. For both 2032 and 18,650 cells, Internal Short Circuit (ISC) defect structures were introduced during cell construction with the electrodes in the as-prepared fully discharged state. Typically, a 1 mm^2 piece of metallic foil (~ 200 μm thick) was fixed to an insulating plastic sheet and placed on the cathode electrode as the potential short-inducing defect (Fig. 1). Cells were heated either in a Tenney environmental chamber or affixed to a brass fixture with heater cartridges controlled using a Solo 5959 temperature controller. The AC cell impedance was monitored at several frequencies during the temperature ramp using an Agilent 4284A LCR impedance analyzer (Agilent Technologies, Inc.) although only 1000 Hz data are shown for clarity.

3. Results and discussion

3.1. Proof-of-concept

Copper electrodes were initially used to determine if a molten metal defect could be used to initiate an ISC in an electrochemical cell. Copper foil electrodes were wound in a cylindrical roll on the 18,650 cell winder with a 1 mm^2 piece of a metal alloy against one electrode and with a pinhole in the insulating separator directly facing the defect structure (to allow for direct electrical contact between the electrodes). The alloy used for these experiments was a Bi/Sn/In alloy with a melting point of ~60 °C. The temperature of the sample was increased to greater than the alloy melting temperature at rate of ~5 °C\min while monitoring the total impedance (Z_{total}) between the electrodes (at 1000 Hz). Fig. 2 shows the normalized impedance (Z_{total}/Z_0) as a function of temperature for four alloy/electrode samples. Because of some scatter in the initial impedance values for each sample ($10 < Z_0 < 35\ \Omega$), total impedance data are normalized to the initial impedance value (Z_{total}/Z_0) for each sample. The impedance slightly decreases with increasing temperature until 58–60 °C, when the impedance drops abruptly to ~100 mΩ (a normalized value of <0.03). This suggests a short between the two copper electrodes triggered by the liquid metal above the melting point. Post-test visual inspection of the unwound roll at ambient temperature showed metal alloy in contact with both electrodes, which was confirmation

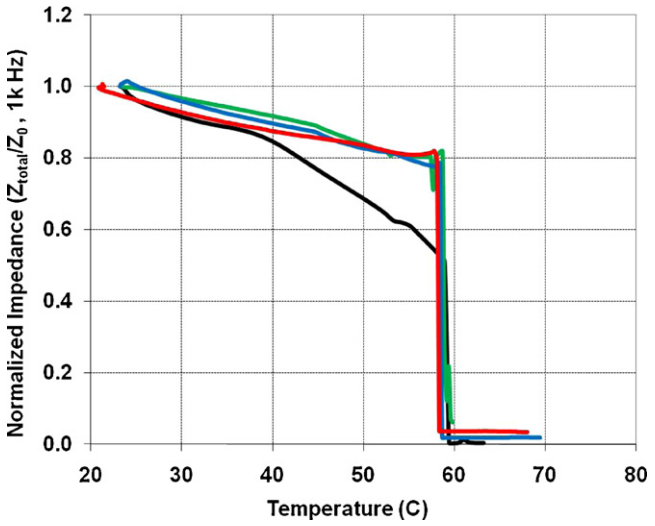

Fig. 2. Normalized total impedance (Z_{total}/Z_0) and a function of temperature for four samples of copper foil electrodes rolled with the ISC alloy defect structures.

that the impedance data supports shorting between the electrodes.

3.2. Studies in 2032 coin cells

The first demonstration of this approach to trigger an ISC in an electrochemical cell was performed in 2032 coin cells. Coin cells were built by inserting either a 1 mm^2 piece of the Bi/Sn/In alloy or gallium metal defect on an insulating plastic spacer on either the $LiCoO_2$ or $Li(Ni_{1/3}Mn_{1/3}Co_{1/3})O_2$ cathode or the graphite anode. A pinhole was made in the polyolefin separator directly above the defect structure and the cells filled with electrolyte. Cells with both the Bi/Sn/In and gallium metal defect structures cycled at C/10 (ambient temperature) for five charge/discharge cycles showed comparable formation cycle performance and capacity to those without the defect; suggesting that the presence of the defect alloy does not impact the ability to safely formation cycle these cells. However, it is important to note that the possible impact of these defects on cell performance under more rigorous testing for long periods of time has not been investigated.

While monitoring cell open-circuit voltage (OCV) of five samples, the cell temperature was increased to 70 °C, as shown in Fig. 3a. Cells LiCO14 and LiCO15 were tested at 3.9 V, cells LiCO13 and LiCO901 were tested at 4.1 V, and cell NMC08 was tested at 4.3 V. Cell NMC08 had a small area of both the anode and cathode active material cleaned away to expose the aluminum and copper current collectors. For the LiCO cells, where the short was between the anode and cathode active materials, the cells shorted to ~2.5–3.0 V between 60 and 65 °C. For the NMC08 cell, where the short was between the aluminum and copper current collectors, the cell shorted to 1.5 V at 65 °C. While this is a relatively small data set, these preliminary results are consisted with earlier modeling and experimental work that suggest that an internal short circuit between current collectors is more severe than shorts between active materials [5,9]. Fig. 3b shows cell OCV for three cells built with gallium metal defect structures as the cell temperature was increased to 40 °C. Cells were tested at 3.1, 3.7. and 4.3 V and all cells shorted between the active materials (Anode–Cathode). Cells NMC118Ga2 and NMC118Ga3 shorted to <1.0 V, while NMC118Ga4 discharged to 2.9 V after the short was triggered at ~34 °C. The trigger temperature for each of these cells is consistent with the melting temperature of gallium metal (~30 °C). Each of these

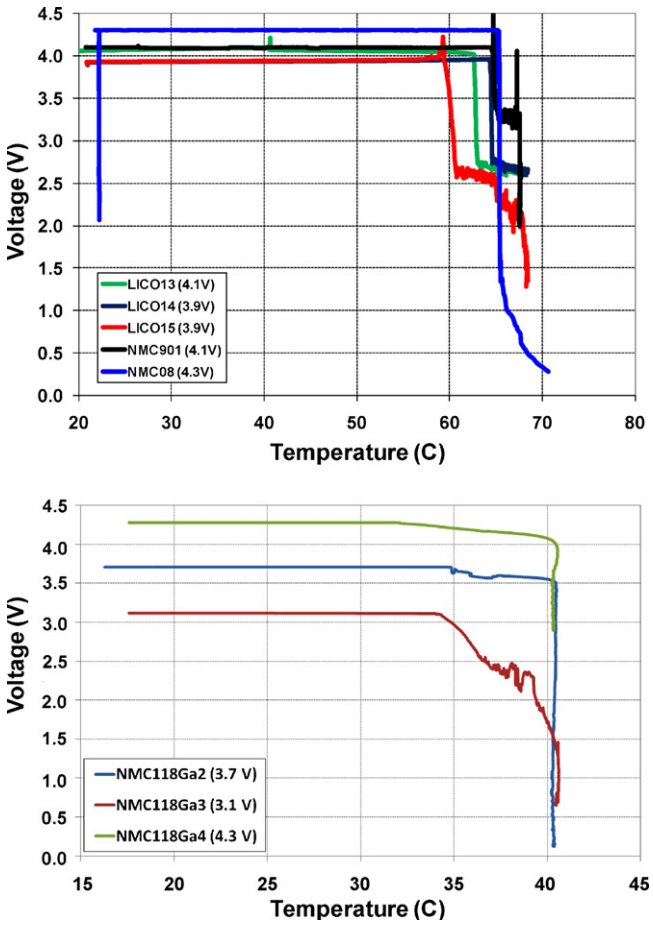

Fig. 3. Cell OCV as a function of temperature for (a) LiCO and NMC coin cells with Bi/Sn/In alloy defect structures and (b) NMC coin cells with gallium metal defect structures showing cell shorting above the melting temperature of the defects (~60 and 30 °C, respectively).

cells discharged to their final voltage over the course of 2–3 min, which is indicative of a moderate resistance short expected for an anode-cathode short.[5,9] Efforts to measure the short resistance during these experiments for different defect structures and types of short circuits (Anode–Cathode, Anode-Al, Cu–Al, etc.) are currently underway and will be the subject of a subsequent publication.

Post-ISC analysis provides additional insight to the mechanism of this ISC trigger. Fig. 4 shows photographs of the electrodes and separators from cell LiCO13. At temperatures >60 °C the alloy had melted and made contact with the cathode electrode which initiated the short. There was also visual evidence that the alloy had

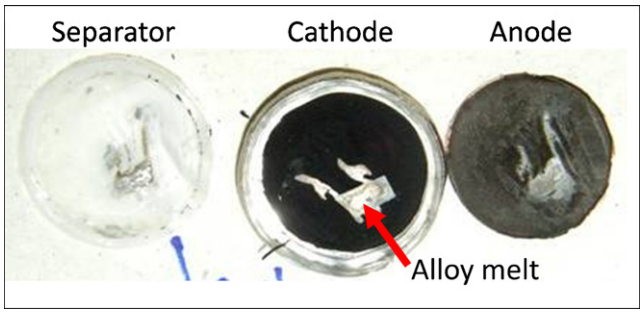

Fig. 4. Photographs of a disassembled coin cell showing the melted alloy foil on the cathode electrode and visual evidence of indium deposited on the separator and the anode electrode.

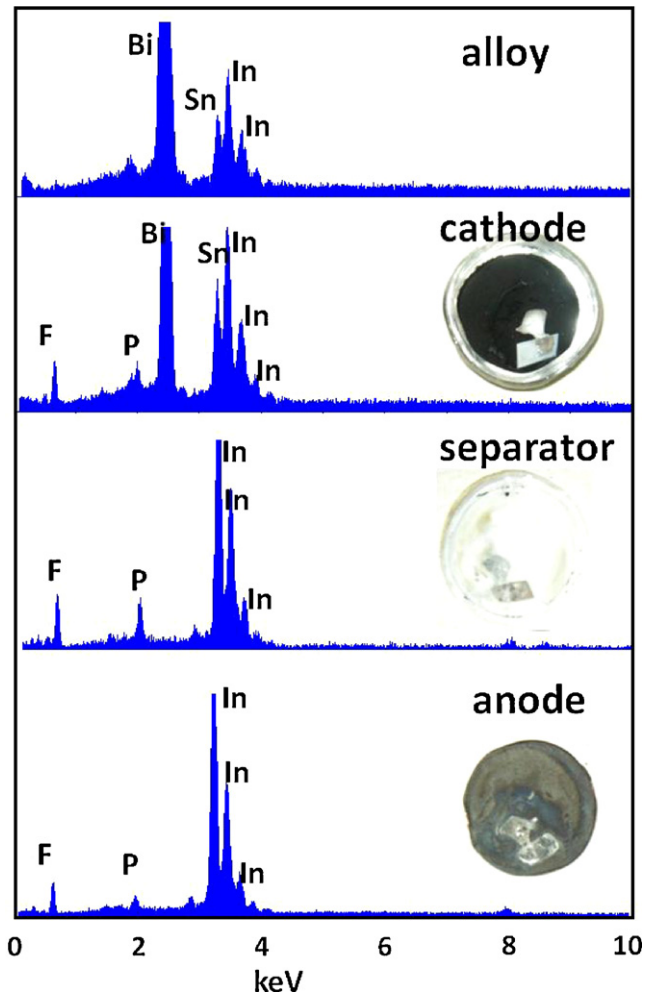

Fig. 5. EDS spectra and corresponding photographs(from top to bottom) of the Bi/Sn/In alloy (control), the alloy on the cathode electrode, indium deposited on the separator, and indium deposited on the anode electrode.

permeated the separator and made contact with anode electrode, which was presumed to have caused the internal short. Fig. 5 shows energy dispersive X-ray spectra (EDS) of each of the metal defect areas on the electrodes and separator of the LiCO14 cell post-ISC, along with a photograph of each cell component. Qualitatively, the EDS spectrum of the melted alloy on the surface of the cathode was largely the same as the control alloy with the addition of phosphorous and fluorine peaks which were contributions from the $LiPF_6$ electrolyte salt. However, the EDS spectra of the metal on the separator and anode were quite different; only showing indium metal along with phosphorous and fluorine from $LiPF_6$. This suggests that only the indium metal from the alloy migrates (and not the Bi/Sn/In eutectic) from the cathode across to the anode and is responsible for triggering the internal short in these cells. Indium metal is known to have a low surface free energy and is used extensively as a solder materials because of its good surface wetting characteristics [12,13]. This supports the observation in this case, where indium preferentially wets the separator and anode surfaces, causing an internal short. It is important to note that EDS is not a technique that is sensitive to low mass elements, including lithium. It is possible that the indium metal that was deposited on the separator and anode causing the internal short likely existed as an indium/lithium alloy [14]. Additional characterization to further elucidate this mechanism of indium migration and possible lithium alloying will be performed and reported at a later date.

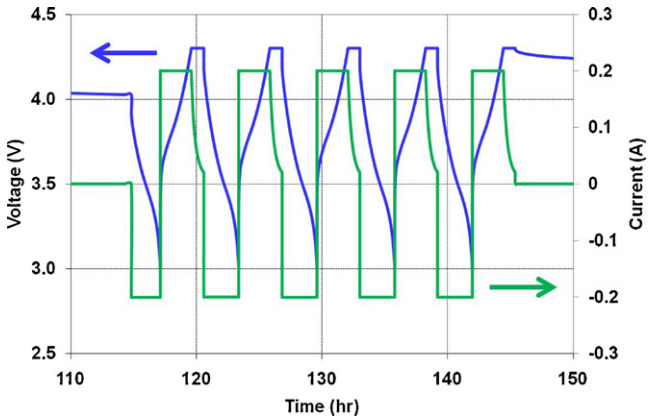

Fig. 6. Formation cycling (C/5 rate) of a representative 18,650 cell built with a Bi/Sn/In defect structure, showing normal cycling behavior.

3.3. ISC demonstration in 18,650 cells

As described for 2032 coin cells, 18,650 cells were also fabricated with alloy defect structures. Typically, 18,650 test cells were built by inserting a 1 mm^2 piece of the Bi/Sn/In alloy defect on an insulating plastic spacer in the middle of the $Li(Ni_{1/3}Mn_{1/3}Co_{1/3})O_2$ cathode electrode. A pinhole was made in the polyolefin separator directly above the defect. The electrodes were rolled using one of the commercial winders and then filled with electrolyte and sealed in an Ar glove box. Fig. 6 shows formation cycling (five cycles) for an 18,650 cells with a Bi/Sn/In alloy defect. Cells built with defect structures showed normal formation cycling at a C/5 rate (0.2 A charge and discharge) and no aberrations or anomalies due to the defect structures.

Internal shorts were triggered in the 18,650 test cells by heating them in a brass heater fixture above 60 °C (above the melting point of the alloy). Fig. 7 shows cell voltage as a function of temperature for an 18,650 cell with a Bi/Sn/In defect structure. At 68 °C, the cell clearly showed an abrupt drop in cell voltage, followed by further instabilities in the cell voltage >70 °C, suggesting a soft (high resistance) internal short. It is important to note that previous work from this Laboratory has shown that the internal temperature of an 18,650 cell can lag behind the cell external skin temperature as much as 10–15 °C when a cell is heated externally. Therefore, the observation of cell shorting at cell skin temperatures between 68 and 75 °C was consistent with an internal cell temperature of ~60–65 °C (melting point of the alloy) and with the short circuit triggered by the melting alloy as observed in the 2032 coin cells.

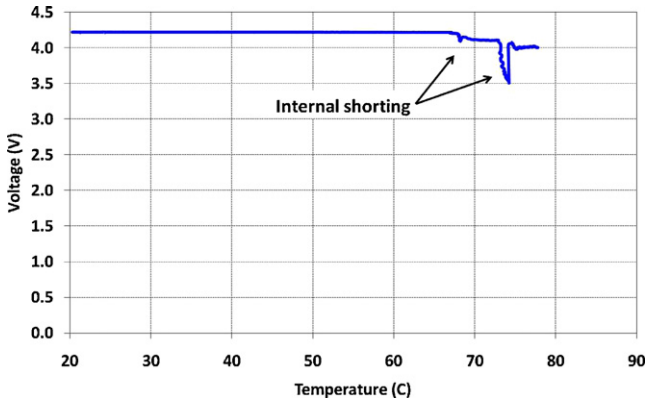

Fig. 7. Cell OCV as a function of temperature for an 18,650 cell built with an ISC defect showing a soft short above the melting temperature of the Bi/Sn/In alloy (~60 °C).

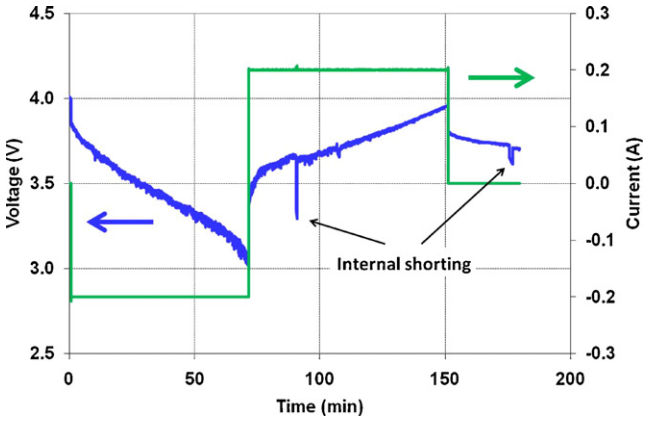

Fig. 8. 18,650 cell cycling (C/5 rate) after the cell was heated to 70 °C to trigger the short defect and cooled to ambient temperature showing evidence of cell damage and soft shorting.

After the short was triggered at elevated temperature, the cells were cooled to ambient temperature and cycled at a C/10 rate to determine the post-test cell state-of-health (Fig. 8). Comparison of the cell cycling data for the same cell before (Fig. 6) and after the internal short was triggered (Fig. 8) showed that the cell voltage profile was stable before the short and very erratic after the short. This is a clear indication of cell damage due to a soft short developed in the cell during this experiment although no thermal runaway or temperature excursion was observed.

4. Conclusion

This report describes a novel approach to triggering internal short circuits in lithium-ion cells of different formats (cylindrical wound and stacked coin cell) without the use of any mechanical deformation of the cell packaging. The trigger in these experiments was a low melting point metal or metal alloy defect that was electrically isolated when the defect was solid but made electrical contact with both electrodes within a cell in the liquid state. While this approach does require heat as the environmental parameter to initiate the short, the trigger temperatures are modest (34–40 °C for gallium and 60–75 °C for Bi/Sn/In) relative to the stability of lithium-ion battery materials. This report highlights the feasibility of this approach in the preliminary experimental work. While the reproducibility of this approach is good in 2032 coin cells, with >80% of cells tested triggered an internal short; reliability and reproducibility of this approach in wound 18,650 cells needs improvement. Specifically, the contact or interfacial resistance between the defect and the electrodes remains a critical barrier to reliably triggering internal short circuits using this technique. Work is continuing on this front to minimize the contact resistance of the short defect, to examine other low melting point metal defects, as well as other thermally labile defect structures to cause internal short circuits in cells. Work is also continuing to improve the reproducibility of this approach and to test the various types of internal shorts (Al–Cu, Cathode-Cu, Anode-Al, etc.) in 18,650 and prismatic cells to determine their thermal response to each type of short. These experimental data will feedback into numerical models for validation and into design of new materials and systems to mitigate the potentially catastrophic effects of a cell failure due to an internal short circuit.

Acknowledgements

The authors gratefully acknowledge M. J. Russell and L. E. Davis for their technical contributions with cell building and testing. This work was performed under the auspices of DOE FreedomCAR and Vehicle Technologies Office. Sandia National Laboratories is a multi-program laboratory managed and operated by Sandia Corporation, a wholly owned subsidiary of Lockheed Martin Corporation, for the U.S. Department of Energy's National Nuclear Security Administration under contract DE-AC04-94AL85000.

References

[1] E. Darcy, J. Power Sources 174 (2007) 575–578.
[2] J. Zhang, S. Santhagopalan, P. Ramadass, IMLB-2008 Tianjin China, Abstract 74.
[3] B. Barnett, D. Ofer, B. Oh, R. Stringfellow, S.K. Singh, S. Sriramulu, J. IMLB-2008 Tianjin China, Abstract 75.
[4] G.-H. Kim, A. Pesaran, R. Spotnitz, J. Power Sources 170 (2007) 476–489.
[5] S. Santhanagopalan, P. Ramadass, Z. Zhang, J. Power Sources 194 (2009) 550–557.
[6] J. Jeevarajan, IECEC 2010 Nashville, TN.
[7] H.P. Jones, J.T. Chapin, M. Tabaddor. "Critical Review of Commercial Secondary Lithium-Ion Battery Safety Standards" 4th IAAS Conference Making Safety Matter (2010).
[8] A. Wu, J.T. Chapin, "Blunt Nail Crush Internal Short Circuit Lithium-Ion Cell Test Method," NASA Battery Workshop (2009).
[9] H. Maleki, J.N. Howard, J. Power Sources 191 (2009) 568–574.
[10] R. Stringfellow, D. Ofer, S. Sriramulu and B. Barnett, 218th ECS 2010 Las Vegas, NV, Abstract 322.
[11] G. Nagasubramanian, Int. J. Electrochem. Sci. 2 (2007) 913–922.
[12] A. Singh, D.A. Horsley, M.B. Cohn, A.P. Pisano, R.T. Howe, IEEE J. Microelectromech. Syst. 8 (1999) 27–33.
[13] C.J. Orendorff, J.M. Barker, A.M. Rowen, W.G. Yelton, C.L. Arrington, J.R. Gillen, SPIE Proc. 7039 (2009), 70390R-1-70390R-11.
[14] J. Sangster, in: T.B. Massalski (Ed.), Binary Alloy Phase Diagrams, 2nd ed., 1990.